Broad scale deformation across the Pacific-North America boundary in Northern California

By

William H. Prescott and David Manaker

U.S. Geological Survey

345 Middlefield Road, MS/977

Menlo Park, CA 94025-3591

Contact: wprescott@usgs.gov

Abstract

Using campaign and continuous GPS data in Northern California collected over the past few years, we can place some constraints on both the San Andreas fault zone deformation and on the North America/Sierra Nevada-Great Valley/Pacific relative plate motion. We examined the motion of 30 stations extending from the Farallon Islands off the coast of California near San Francisco to the Sierra Nevada foothills observed over the time period 1992 to 1999. Using a two-dimensional model, we estimated the N33.9˚W component of velocity of the Sierra Nevada-Great Valley microplate and the slip rates on San Andreas system faults. There is no evidence of significant motion normal to this direction, the direction of the Pacific-North America rotation vector at the Farallon Islands. The Sierra Nevada-Great Valley microplate appears to behave rigidly and is moving at 10.9±0.4 mm/a relative to North America. West of the Sierra Nevada-Great Valley microplate, the San Andreas fault system absorbs an additional 39.8±2.3 mm/a across a zone that is about 100 km wide (at the latitude of San Francisco). The motion is best fit by a model with 20.6±1.1 mm/a slip on the San Andreas fault, 8.5±1.6 mm/a on the Rodgers Creek fault and 10.7±1.3 mm/a on the Green Valley fault. Standard deviations are one sigma. Within the uncertainties, these geodetically-derived loading rates are not inconsistent with geologic estimates for the fault slip rates. However, the geodetic results suggest a higher-than-geologic rate for the Green Valley and lower-than-geologic rate for the Rodgers Creek fault.

Introduction

Northern California is located on the boundary between the North American plate and the Pacific Plate. Between rigid North America and the Pacific plate there are three tectonic provinces with distinct styles by which they accommodate the relative motion of North America and Pacific. There is a broad region of distributed deformation, the Great Basin, [*Bennett et al.*, 1998],[*Thatcher et al.*, 1999], accommodating about 1 cm/a of the Pacific-North America motion. There is the San Andreas system, a zone of right lateral shear, about 100 km wide and accommodating some 4 cm/a. Between them, there is a relatively rigid micro-plate, the Sierra Nevada-Great Valley, [*Argus and Gordon*, 1991a]. It has long been recognized that motion on the San Andreas system did not account for all of Pacific-North America motion [*Atwater*, 1970]. Space geodetic techniques allow relative ground velocities to be determined over hundreds and thousands of kilometers. These observations supplement the detailed local measurements that have been made along the San Andreas shear zone over the past three decades. In this paper we examine the velocities of geodetic stations distributed across the San Andreas shear zone in Central California and across the Sierra Nevada-Great Valley microplate. These observations place strong constraints on the nature and distribution of motion in these two tectonic provinces.

Data

During the past few years, a consortium of institutions in Northern California (University of California, Berkeley, U.S. Geological Survey, University of California, Davis, Stanford University, and Trimble Navigation) have installed and operated continuous Global Positioning Systems (GPS) receivers at fixed sites in northern and central California. This Bay Area Regional Deformation (BARD) spans the Sierra Nevada-Great Valley micro-plate, the San Andreas system and the edge of the Pacific plate (Fig.1). We have analyzed about 5 years of data sampled from the continuous records at Bay Area Regional Deformation (BARD) sites in north-central California (Fig.1). The size of the array has grown from 2 stations in the early 1990's to its present configuration of about 28 stations. In addition we have examined data from several profiles across the Bay area that have been observed in campaign mode over the time period 1992 to 1999 (Fig.2).

All of the GPS data were processed with GIPSY software [*Zumberge et al.*, 1997] in a "point positioning mode" using clocks and orbits from the NASA/Caltech Jet Propulsion Laboratory. After point positioning all of the stations, local and tracking, ambiguities for the local stations were resolved in a network processing mode. The processing produces loosely constrained positions for all of the BARD stations and for a subset of the International GPS Service stations (Fig. 2). The processing was done using daily bins of the observed phase data. Each processed-day resulted in position file containing coordinates for all of the observed local stations plus some subset of the IGS tracking stations. Because these solutions are not tied to any reference frame, the position of a station varies from epoch to epoch as a result of reference frame uncertainties in addition to any station motion. In order to obtain velocities relative to "Stable North America", we removed this reference frame uncertainty as follows. We started with ITRF96 positions and velocities [*Boucher*, 1997; *Boucher et al.*, 1996] for the IGS stations in Fig. 3. These velocities are essentially in a NUVEL1-NNR motion [*Argus and Gordon*, 1991b] reference frame. We used the ITRF96 velocities for 7 tracking stations (ALGO, BRMU, DRAO, FAIR, NLIB, PIE1, YELL) to determine an Euler pole for the motion of these stations relative to Nuvel-NNR1A. This Euler pole has the components: 2.5˚ North, -82.5˚ East, 0.211˚/ma. The predicted motion about this Euler pole was subtracted from all of the tracking stations. This produced a "North America-fixed" reference frame. Finally, each epoch solution for the local positions+IGS stations was rigidly rotated and translated (7-parameter-Helmert-transformed) into the configuration that most closely approximated the reference frame. The result of this process is a series of positions for each station relative to "fixed" North America. A typical example of the time series is shown in Fig. 3. The BARD stations operate continuously. However, in order to reduce the processing time required, we have generally only processed one solution per week. Weekly solutions provide more than enough data to provide estimates of the velocities. In the case of profile stations observed in campaign-mode, all of the data were processed. Typically, these stations are observed on 2 consecutive days, once a year. Repeatability can best be judged from the continuous stations. We estimate repeatability from the RMS residual about the best fit to the time series for a single station assuming that changes in the position are linear with time. We find that station components have a typical repeatability of about 3, 5, and 15 mm in the north, east and up components respectively. All of the errors used in this discussion are derived as follows: we start with the formal errors obtained in the GIPSY solutions. These are scaled to produce a scaled-formal-error level that approximates the observed RMS about the linear fit to the time series. The scaling factors used are 3.0, 4.0 and 3.0 for the north, east and up components. Errors in the velocities are then calculated by assuming that there are two sources of error in the velocities. The first source is gaussian and is estimated from the scaled-formal-errors (propagating them through the velocity calculation). The second source is a random walk. Based on no data, we assume that the random walk component is 1.0 $mm/a^{1/2}$. Without some other source of error, the assumption that the errors are gaussian produces estimates of the velocity error that are clearly too small, particularly for long, frequently-observed time series.

Discussion

In Fig. 4 and Table 1, we resolve the motion of the stations into components parallel and normal to the direction of Pacific-North America plate motion [*Argus and Gordon*, 1991b] at San Francisco (N33.85˚W). It is clear from this figure that in the eastern half of the region, the character of the deformation is very different than that in the western half of the region. The eastern stations span a region that has been called the Sierra Nevada-Great valley microplate, while the western stations span a complex region including several major strike slip faults, all part of the San Andreas shear zone. In both sections, the motion normal to the plate motion direction is much smaller.

Sierra Nevada-Great Valley microplate rate

The seven most northeasterly stations share a common motion, that of the Sierra Nevada Great Valley microplate. There is little evidence of deformation within the region spanned by the stations (Table 2) Quincy (QUIN), Columbia (CMBB), Davis (UCD1), Musick Mountain (Shaver Lake) (MUSB), Orville (ORVB), Sutter Buttes (SUTB), and Owens Valley Radio Observatory (OVRO). The observations at these stations are consistent with the notion of a rigid Sierra Nevada Great Valley microplate.

San Andreas shear zone deformation

The GPS stations form a profile that crosses the San Andreas shear zone at the northern end of San Francisco Bay. At this latitude the principal faults comprising the shear zone are the Green Valley, Napa. Rodgers Creek and San Andreas. Other studies have examined the distribution of motion in this area [*Lisowski et al.*, 1991; *Prescott and Yu*, 1986]. Geologic investigations [Lienkaemper, personal communication] suggest that the San Andreas, Rodgers Creek and Green Valley faults have significant rates of motion over the past few thousand years.

In analyzing the geodetic results, we tried to reduce the model uncertainties as much as possible so that the questions that remained could be answered with confidence.

To this end, we made the following assumptions:

- The crust behaves as a linear elastic half space;
- The faults are locked at the surface and slipping below some depth;
- The locking depths are known and agree with depth of seismicity as given by[*Williams*, 1995];
- The active faults are San Andreas, Rodgers Creek and Green Valley; and
- Rigid motion of the entire profile (translation) relative to North America is a consequence of Sierra Nevada Great Valley motion.

We used a 2 dimensional model for the faults [*Chinnery*, 1961]. The faults were treated as infinite screw dislocations at prescribed locations and depths. We also experiment with models that included locking depth or fault location as free parameters. The used a non-linear inversion routine for all the calculations. However, the fault depth and locations tended to be highly correlated with slip rate. Models that included both slip rate and location as unknowns, produced slip rates that were very uncertain. We decided to constrain the fault locations and locking depths based on other evidence and focus on resolving the slip rates at depth. With constraints on the location of the slip surface, slip rates at depth on the three faults were well resolved by the model. The best fitting model is given in Table 2 and shown in Figure 5. The results of this model are consistent with geologic estimates of the slip rates (shown in Table 2, as well). However, this model implies a Pacific-North America plate motion rate (50.3±2.7 mm/a) that is slightly higher than either NUVEL1 (48.7 mm/a) or NUVEL 1A (46.7 mm/a) at this latitude[*Argus and Gordon*, 1991b; *DeMets et al.*, 1994]. The model provides an excellent fit to the observations. It fits all of the observations within one standard deviation. The overall estimated variance is 1.2 indicating that almost all of the model misfit is attributable to the uncertainty in the observations.

We also tried constraining the model by requiring that the total motion agree with NUVEL 1A. These results are shown in Table 3 and Figure 6. With this constraint it is not possible to fit the western-most observations (Farallon Islands and Point Reyes Head). In order to keep the overall motion within the limit, the model reduces the slip on the San Andreas fault (probably because this fault is the least constrained, with few observations to the west). It also produces a geodetic rate on the San Andreas fault (16.7±0.9 mm/a) that is significantly lower than the geologic rate (23 mm/a). Note that the geologic slip rates give about the right shape to the distribution (Figures 5 and 6) but the geologic curve lies below all of the observations (a consequence of the fact that the geologic rate on the Green Valley fault is lower than the observations require). The constrained solution of Figure 6 and Table 3 is a significantly worse fit to the data.

Table 4 and 5 compare the motion of the Pacific plate relative to North America and relative to the Sierra Nevada Great Valley for various recent determinations. The rates obtained from our fault motion inversion seem very consistent with recent determinations of the rates from more distant stations.

Table 1. Observed station velocities.

Name	Normal position (km)	Parallel (mm/yr)	Normal (mm/yr)	Par-std (mm/yr)	Norm-std (mm/yr)
FARB	-40.9	48.39	-2.73	0.6	0.6
PRH3	-23.2	46.28	-0.75	1.1	1.3
PRNC	-11.8	40.78	-1.38	1.7	2.0
PRH2	-9.0	41.33	-0.67	1.0	1.1
1395	-5.1	39.61	-2.99	1.1	1.2
PRSD	-0.3	32.55	-1.32	1.1	1.3
NICC	0.0	36.50	0.22	1.2	1.4
PBL1	4.8	32.64	-7.95	0.7	0.7
TIBB	5.4	33.00	-1.57	0.6	0.6
NAVY	5.4	32.94	-1.46	1.1	1.3
MOLA	10.6	31.88	-0.83	0.8	0.8
CORD	14.5	29.72	0.08	0.9	1.0
UCBK	15.5	30.02	-1.90	1.4	1.5
ADOO	21.9	28.07	-0.27	1.2	1.3
AIRR	25.4	27.13	-0.23	1.1	1.3
DEAL	34.9	21.13	-1.94	3.9	4.3
HENN	35.1	19.77	-0.52	2.0	2.4
HAGG	43.9	21.02	-1.83	1.3	1.4
MADI	46.7	18.92	-1.92	1.6	1.7
GAME	50.8	16.84	-2.78	1.2	1.4
GORR	53.3	19.09	-3.34	1.4	1.6
VAC3	58.2	21.04	0.87	3.9	4.2
CAML	66.1	13.99	-1.96	1.3	1.5
UCD1	88.6	11.93	0.50	1.0	1.0
SUTB	125.8	9.41	-3.40	1.2	1.3
CMBB	142.1	12.64	-4.42	0.6	0.6
MUSB	155.2	10.82	-0.88	1.7	1.8
ORVB	167.3	10.30	-4.24	1.0	1.0
OVRO	222.5	11.64	5.25	4.5	5.0
QUIN	227.8	12.26	-2.50	0.6	0.6

Table 2. Preferred Model. Unconstrained Solution (Estimated variance = 1.3)

Fault	Depth	Rate	Std Err	Conf.	Interval	Geol. rate
	km	mm/a	mm/a	mm/a	mm/a	mm/a
SA	12.2	22.8	1.2	20.3	25.4	23
RC	8.5	7.1	1.8	3.5	10.7	10
GV	10.5	10.7	1.5	7.6	13.8	7
SNGV		10.7	0.4	9.9	11.5	(10.7)
Total		50.3	2.7			51

Table 3. Constrained Solution (Estimated variance = 2.9)

Fault	Depth	Rate	Std Err	Conf.	Interval	Geol. rate
	km	mm/a	mm/a	mm/a	mm/a	mm/a
SA	12.2	16.7	0.9	14.8	18.6	23
RC	8.5	9.7	2.5	4.5	14.8	10
GV	10.5	10.2	2.2	5.7	14.7	7
SNGV		10.1	(Inferred)			(10.1)
Total		46.7	(Constrained)			51

Table 4. Comparison of North America-Pacific rates.

Source	Rate	Std Err	Dir	Std Err
	mm/a	mm/a	Degrees NW	Degrees
Nuvel-1[1]	48.7	0.5	33.8	0.5
Nuvel-1A[2]	46.6	0.5	33.8	0.5
A-G 1999[3]	49.9	0.4	35.8	0.4
D-D 1999[4]	50.1	0.4	35.9	0.4
P 1999[5]	50.3	2.7	33.8	

Notes 1. [*Argus and Gordon*, 1991b]
2. [*DeMets et al.*, 1994]
3. [*Argus and Gordon*, 1999]
4. [*DeMets and Dixon*, 1999]
5. This paper

Table 5. Comparison of Sierra Nevada Great Valley-Pacific rates.

Source	Rate	Std Err	Dir	Std Err
	mm/a	mm/a	Degrees NW	Degrees
A-G 1999[1]	40.0	3.6	35.8	0.4
P 1999[2]	40.6	2.6	33.8	

Notes 1. [*Argus and Gordon*, 1999]
2. This paper

Conclusions

We find no evidence for deformation within the Sierra Nevada Great Valley block located between the Pacific and North America plates. This microplate appears to be moving 10.7±0.4 mm/a relative to stations on the North America plate.

The geodetic observations imply that the seismogenic portions of the San Andreas, Rodgers Creek, and Green Valley faults are currently being loaded at rates of 22.8±1.2, 7.1±1.8 and 10.7±1.5 mm/a, respectively.

Within the uncertainties, these geodetically-derived loading rates agree with geologic estimates for the fault slip rates. However, the geodetic results suggest a higher-than-geologic rate for the Green Valley and lower-than-geologic rate for the Rodgers Creek fault.

Collectively, the Sierra Nevada Great Valley motion plus all the fault slip rates suggest that the Pacific-North America motion occurs a higher rate than the NUVEL-1 or -1A rate.

We chose to examine the slip budget at the northern end of San Francisco Bay because at this latitude the faults are relatively well separated and the deformation is less complicated by along-strike variations, particularly in near surface creep rates. However, we would argue that these results also provide the best constraints available for faults farther south, (i.e. the Hayward and Calaveras faults). To a lesser degree this is also true for the San Andreas fault along the San Francisco peninsula. However, this latter inference is complicated by the presence of the San Gregorio fault which appears to merge with the San Andreas between the area covered by this study and the peninsula.

References

Argus, D.F., and R.G. Gordon, Current Sierra Nevada-North America motion from very long baseline interferometry: Implications for the kinematics of the Western United States, *Geology*, *19*, 1085-1088, 1991a.

Argus, D.F., and R.G. Gordon, No-net rotation model of current plate velocities incorporating plate motion model NUVEL-1, *Geophysical Research Letters*, *18* (11), 2039-2042, 1991b.

Argus, D.F., and R.G. Gordon, Present tectonic motion across the Coast Ranges and San Andreas Fault System in Central California, *Geological Society of America Bulletin*, *submitted*, 1999.

Atwater, T., Implications of plate tectonics for the Cenozoic tectonic evolution of western North America, *Geological Society of America Bulletin*, *81*, 3513-3536, 1970.

Bennett, R.A., B.P. Wernicke, and J.L. Davis, Continuous GPS measurements of contemporary deformation across the northern Basin and Range province, *Geophys. Res. Lett.*, *25* (4), 563-566, 1998.

Boucher, C., ITRF96, http://lareg.ensg.ign.fr/ITRF/itrf96.html, 1997.

Boucher, C., Z. Altamini, M. Feissel, and P. Sillard, Results and analysis of the ITRF94, Observatoire de Paris, Paris, 1996.

Chinnery, M., Deformation of the ground around surface faults, *Bulletin of the Seismological Society of America*, *51*, 1961.

DeMets, C., and T.H. Dixon, New kinematic models for Pacific--North America motion from 3 Ma to present, 1, Evidence for steady motion and biases in the NUVEL-1A model, *Geophysical research letters*, *26* (13), 1921, 1999.

DeMets, C., R.G. Gordon, D.F. Argus, and S. Stein, Effect of recent revisions to the geomagnetic reversal timescale on estimates of current plate motions, *Geophysical Research Letters*, *21* (20), 2191-2194, 1994.

Lisowski, M., J.C. Savage, and W.H. Prescott, The velocity field along the San Andreas fault in central and southern California, *Journal of Geophysical Research*, *96* (B5), 8369-8388, 1991.

Prescott, W.H., and S.-B. Yu, Geodetic measurement of horizontal deformation in the Northern San Francisco Bay region, California, *Journal of Geophysical Research*, *91* (B7), 7475-7484, 1986.

Thatcher, W., G.R. Foulger, B.R. Julian, J. Svarc, E. Quilty, and G.W. Bawden, Present-Day Deformation Across the Basin and Range Province, Western United States, *Science*, *283* (5408), 1714-1718, 1999.

Williams, S.D.P., Current motion on faults of the San Andreas System incentral California inferred from recent GPS and terrestrial survey measurements, Ph.D. thesis, University of Durham, Durham, England, 1995.

Zumberge, J.F., M.B. Heflin, D.C. Jefferson, M.M. Watkins, and F.H.Webb, Precise point positioning for the efficient and robust analysis of GPS data from large networks, *Journal of Geophysical Research*, *102* (B3), 5005-5018, 1997.

Figure Captions

Figure 1. Map and velocity vectors for GPS network. Error ellipses indicate 95% confidence.

Figure 2. Observed time series at the Farallon Island station (FARB). Error bars (+/- one sigma) are shown in faint gray.

Figure 3. Plot of the motion of stations resolved into components parallel and normal to the observed direction of Pacific-North America motion (N33.85˚W). Solid red dots indicate the motion parallel to the direction of plate motion. Solid blue dots indicate the motion normal to the direction of plate motion. The Pacific plate is at the left; the Sierra Nevada plate is at the right. Distance is measured from about San Francisco.

Figure 4. Models. Red: Best fit to geodetic observations with no constraint on total plate motion rate. Green: Slip at geologic rates on San Andreas (24.0 mm/a), Rodgers Creek (8.5 mm/a), and Green Valley (5.0 mm/a).

Figure 5. Models. Red: Best fit to geodetic observations with a constraint of 46.7 mm/a on total plate motion rate. Green: Slip at geologic rates on San Andreas (24.0 mm/a), Rodgers Creek (8.5 mm/a), and Green Valley (5.0 mm/a).

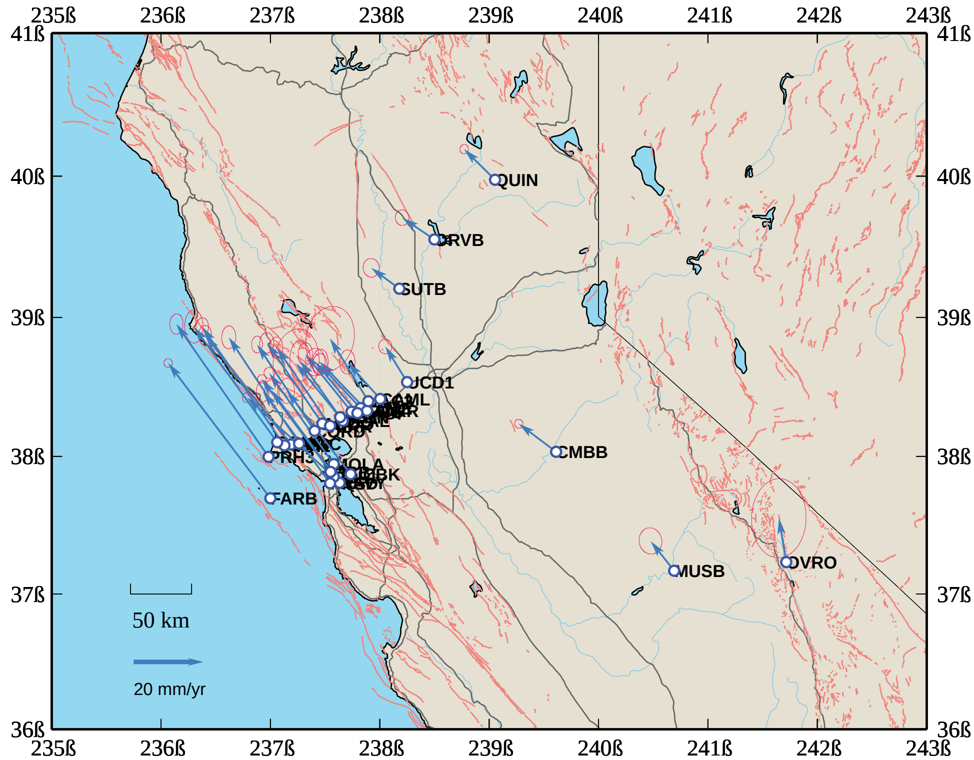

Figure 1. Map of the Global Positioning System stations and velocity vectors. Error ellipses indicate 95% confidence.

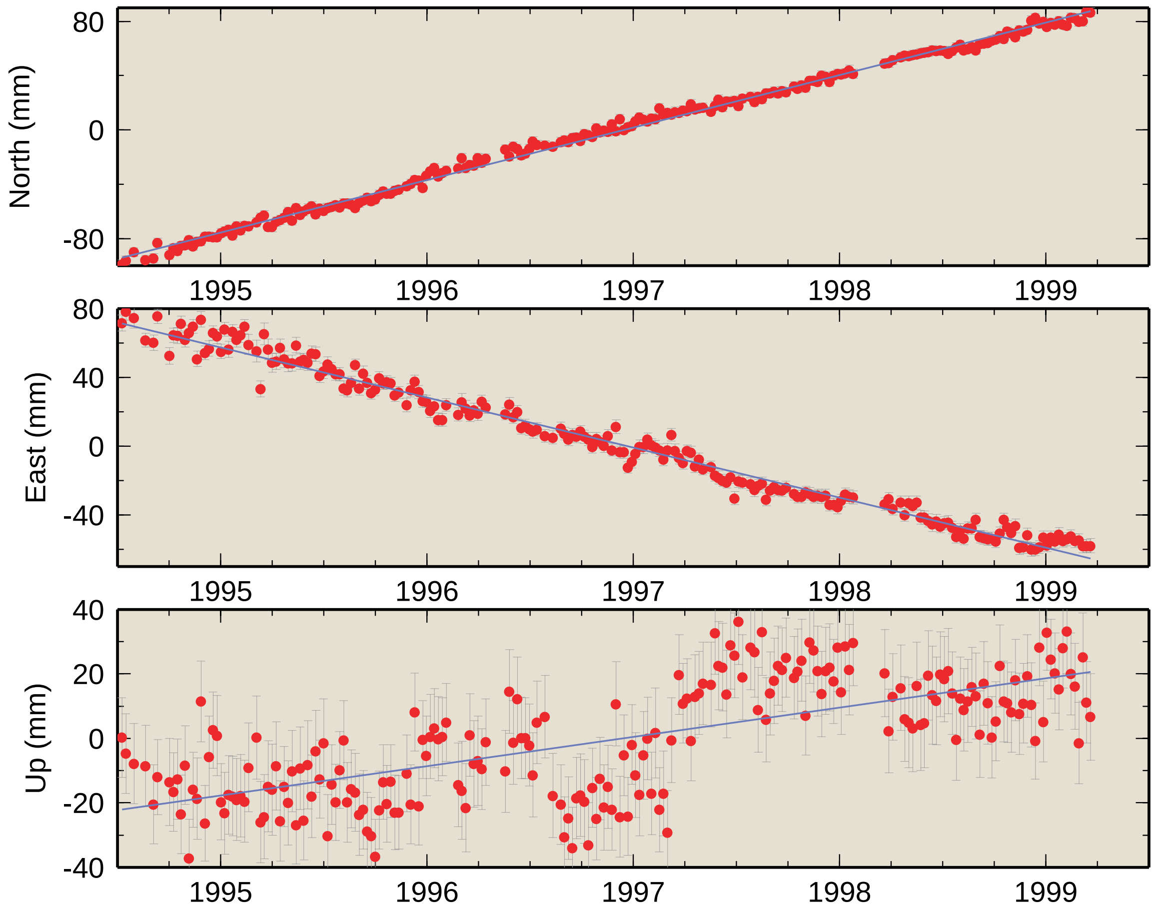

Figure 2. Observed time series at the Farallon Island station (FARB). Error bars (+/- one sigma) are shown in faint gray.

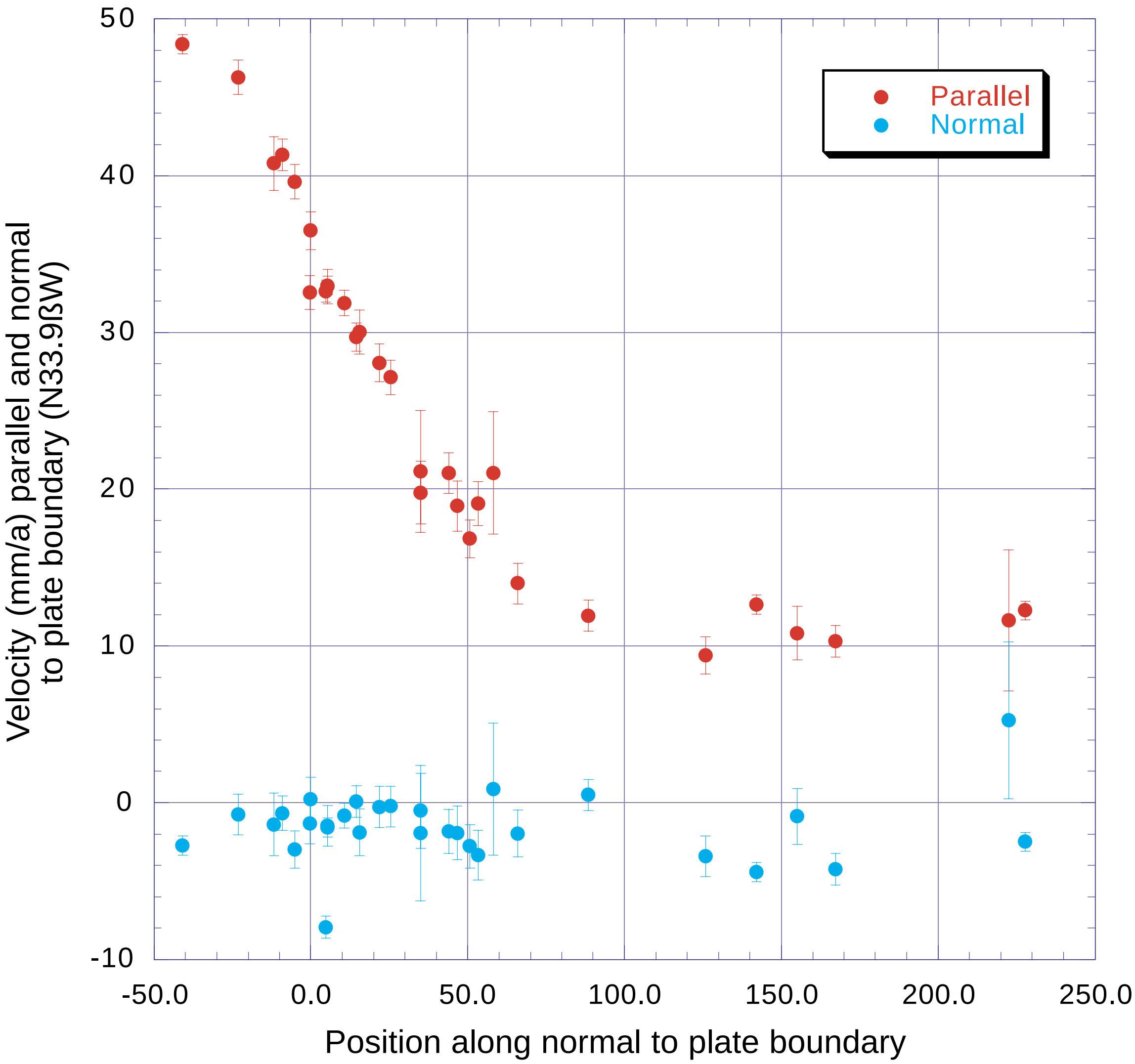

Figure 3. Plot of the motion of stations resolved into components parallel and normal to the observed direction of Pacific-North America motion (N33.85˚W). Solid red dots indicate the motion parallel to the direction of plate motion. Solid blue dots indicate the motion normal to the direction of plate motion. The Pacific plate is at the left; the Sierra Nevada plate is at the right. Distance is measured from about San Francisco.

Figure 4. Preferred model. Red: Best fit to geodetic observations with no constraint on total plate motion rate. Green: Slip at geologic rates on San Andreas (24.0 mm/a), Rodgers Creek (8.5 mm/a), and Green Valley (5.0 mm/a).

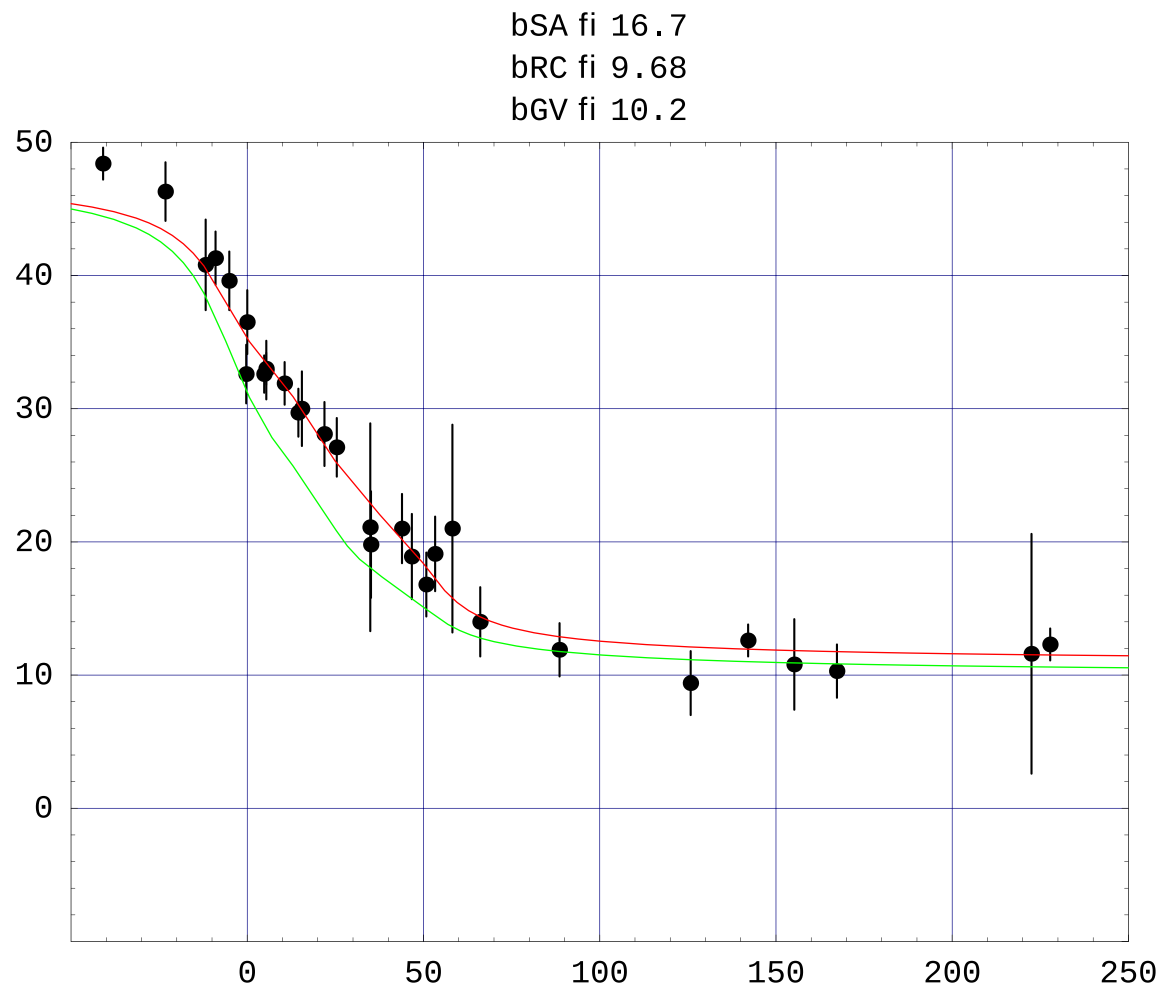

Figure 5. Models. Red: Best fit to geodetic observations with a constraint of 46.7 mm/a on total plate motion rate. Green: Slip at geologic rates on San Andreas (24.0 mm/a), Rodgers Creek (8.5 mm/a), and Green Valley (5.0 mm/a).